JOURNAL OF GUIDANCE, CONTROL, AND DYNAMICS
Vol. 30, No. 5, September–October 2007

Engineering Notes

ENGINEERING NOTES are short manuscripts describing new developments or important results of a preliminary nature. These Notes should not exceed 2500 words (where a figure or table counts as 200 words). Following informal review by the Editors, they may be published within a few months of the date of receipt. Style requirements are the same as for regular contributions (see inside back cover).

Active Suppression of Flutter with a Smart Flap

Ranjan Vepa*
University of London,
London, E1 4NS England, United Kingdom

DOI: 10.2514/1.28152

I. Introduction

THE concept of the typical section is a two-dimensional idealization that allows for the synthesis and design of aeroelastic dynamic and control systems. It is usually modeled as an airfoil suspended by a plunging and by a pitching spring representing the structural dynamics of a typical wing section. Conventional airfoil sections are fitted with ailerons and trailing edge flaps which are generally hinged to the main section. In this study, we employ a continuously flexible flap. The mechanization and actuation of such a flap, a model of which is currently being built and tested at Queen Mary, University of London, is accomplished by employing structurally embedded, multilayered, shape memory alloy actuators and active composites that are programmed to flex the flap into the desired shape. The structure is thus considered to be smart because it uses the sensor information to make decisions about how to modify its shape or other properties to improve the performance of the overall system.

In this paper we consider the problem of active flutter suppression by employing such smart flaps. Could one expect that by introducing such a flexible flap, flutter can be more easily eliminated than by a rigid flap? To answer this question and to analyze the effectiveness of such a "smart" flap it is first intended to employ the flap as a feedback controller with an active feedback control law that is designed to actively regulate the structural vibrational amplitudes of the airfoil and thus suppress the occurrence of the flutter-type instabilities. To be able to actually establish the complete dynamics of a flexible flap airfoil, including significant but minimal aerodynamic vortex, wake, and interaction effects, we establish the idealized, incompressible potential flow based on unsteady aerodynamic generalized force coefficients for such flexible flaps by reconsidering the original work of Theodorsen and Garrick [1], in relation to hinged flaps.

It is assumed that the continuous deflection of such flaps may be affected by means of a distribution of control effectors. It is further assumed that modal set point commands can be translated into a set of individual set point commands to these distributed actuators which would in turn deform the flap as in the desired mode. Such an assumption is now known to be valid for structures actuated by shape memory alloy (SMA) wire bundle actuators, which tend to behave as force-control integrators in the open loop. The methodology of optimal control is employed to obtain the relevant multi-input–multi-output optimal regulation control laws and the relevant command signals that are needed to drive the actuators.

Although it is always possible to model a flexible flap by a hinged rigid flap and tab combination, which has been thoroughly and completely studied by Nissim [2], there is sometimes a need to focus on the essential differences between a flexible and a rigid articulated flap. As pointed out by Theodorsen and Garrick [1] themselves, the latter suffers from a singularity in the pressure distribution at the leading edge of the flap. Although this does not significantly affect the hinge moment acting on the flap (or tab), it is important to ensure that its absence does not cause any detrimental effects in a flexibly actuated flap. This study shows that, while a flexible flap mode may not be as effective as a rigid hinged flap, the ability to deploy several control modes more than compensates the shortcomings. In fact, the multimode feature is an important aspect that is absent in a rigid flap. In a sense, the flexible flap is a natural generalization of the flap–tab combination.

II. Dynamic Model

The model adopted for our study is the typical section with a flexible flap. The flap is assumed to be a cantilevered beam, attached to the main wing along a seamless hinge line. Along the hinge line the cantilevered flap is assumed to satisfy the boundary conditions of a rigidly fixed beam of zero displacement and slope. In order to establish the dynamic equations of motion, the total kinetic energy of the typical airfoil section is obtained. To this end the vertical downward displacement of any mass point in the section is expressed in terms of the plunging displacement h, and the section pitch angle a about the elastic axis. The flap motion is described in terms of a finite number of assumed mode shapes, $\phi_i(\xi)$, $i = 2, 3, \ldots, N$, where ξ is a nondimensional coordinate directed toward the trailing edge of the flap and the corresponding modal displacement amplitudes, β_i. Typically for a rigid airfoil pitching about midchord, the first two modes are the pure plunging and the pitching modes. We model the flap as a nonuniform cantilevered beam, fixed rigidly to the airfoil main section which is itself assumed to be rigid. For a cantilevered flexiflap, fixed at $\xi = \xi_h$ and free at $\xi = 1$, the following airfoil mode shapes are relevant:

$$\phi_0(\xi) = 1, \qquad \phi_1(\xi) = \xi \tag{1a}$$

$$\phi_i(\xi) = \left(1 - 2\left(\frac{i-1}{i+1}\right)\frac{(\xi-\xi_h)}{(1-\xi_h)} + \frac{i(i-1)}{(i+1)(i+2)}\frac{(\xi-\xi_h)^2}{(1-\xi_h)^2}\right) \times (\xi-\xi_h)^i, \quad i = 2, 3, 4, \ldots, N \tag{1b}$$

where $\xi \geq \xi_h$.

Employing the Lagrangian method, we may write the Euler–Lagrange equations as

$$\mathbf{M}_s\ddot{\mathbf{x}} + \mathbf{K}_s\mathbf{x} = (\mathbf{F}_{\mathrm{AG}} + \mathbf{F}_C)/m \tag{2}$$

where the state vector $\mathbf{x}$ is defined as $\mathbf{x} = [h/b \;\; \alpha \;\; \beta_1 \;\; \cdots \;\; \beta_n]^T$, $\mathbf{F}_{\mathrm{AG}}$ is the generalized aerodynamic force vector, $\mathbf{F}_C$ is the vector of the corresponding control forces and moments, $\mathbf{M}_s$ is the structural inertia matrix, and $\mathbf{K}_s$ is the structural stiffness matrix.

Received 3 October 2006; revision received 4 June 2007; accepted for publication 4 June 2007.

*Lecturer, Department of Engineering, Queen Mary, Mile End Road; R.Vepa@qmul.ac.uk.

In this study we restrict our attention to unsteady incompressible flow with the underlying assumption that the flight is essentially low speed. To derive the generalized aerodynamic forces and moments on the airfoil including the effects of the flexible flap, we consider the expression for the nondimensional pressure coefficient as given by Ashley and Landahl [3]. The nondimensional pressure coefficient is given as

$$\Delta C_p(x) = \frac{\Delta p(x)}{(1/2)\rho U^2} = \frac{4}{\pi}\sqrt{\frac{b-x}{b+x}}\int_{-b}^{b}\sqrt{\frac{b+x_1}{b-x_1}}\frac{\hat{w}_a(x_1)}{x-x_1}\,\mathrm{d}x_1 + \frac{4i\omega}{\pi U}\sqrt{(b^2-x^2)}\int_{-b}^{b}\sqrt{\frac{1}{b^2-x_1^2}}\frac{\hat{p}_a(x_1)}{x-x_1}\,\mathrm{d}x_1 + \frac{4}{\pi\times b}[1-C(k)]\sqrt{\frac{b-x}{b+x}}\int_{-b}^{b}\sqrt{\frac{b+x_1}{b-x_1}}\hat{w}_a(x_1)\,\mathrm{d}x_1 \tag{3}$$

where

$$\hat{p}_a(x) = \int_{-b}^{x}\hat{w}_a(x_1)\,\mathrm{d}x_1 = b\int_{-1}^{x/b}\hat{w}_a(x_1)d\left(\frac{x_1}{b}\right) = b\int_{-1}^{x/b}\hat{w}_i(x_1/b)d\left(\frac{x_1}{b}\right) \tag{4}$$

The generalized modal force coefficients may be defined in terms of the nondimensional integral expression,

$$G(\phi_i, c_i, \phi_j, c_j) = \frac{1}{2\pi}\int_{c_i}^{1}\Delta C_p^j(\xi_1)\phi_i(\xi_1)\,\mathrm{d}\xi_1 \tag{5}$$

where c_i, the lower integration limit, is either -1 for a rigid mode or defined by the location of the flap notional hinge line for a flexible mode, representing the line beyond which the flap is assumed to be flexible. Thus we obtain the generalized forces by an assumed mode approach by carefully employing the Gauss–Chebychev quadrature to the singular integrals to obtain their Cauchy principal values.

Employing the Jones approximation for Wagner's indicial function [4], the complete equations of motion of the typical airfoil section with the smart flap may be assembled and expressed in state-space form. The closed-loop actuator dynamics is ignored.

III. Control Law Synthesis

Much of the past work on active flutter suppression is focused on designing a controller for aircraft wing systems, which can be described by a representative model. Although the main thrust of the research has been based on augmented state models, there has also been an interest in frequency domain and nonaugmented state models. The primary objectives for the design of the controller can be addressed when the requirements for the design of an active controller for flutter suppression can be met with uncertain parameter systems subject to unmeasurable disturbances. To meet these objectives the linear quadratic Gaussian method with the loop transfer recovery (LQG/LTR) design method is adopted which is based on the linear quadratic regulator (LQR) design coupled with the Kalman filter. Thus, the first step in the design is the synthesis of a LQR-type controller followed by the selection of the Kalman filter gain, $\mathbf{L}$.

The final step in the LQG/LTR design is to choose the free design parameters ($\mathbf{Q}$ and $\mathbf{R}$, the state and control weighting matrices in the quadratic performance cost function) such that the LQG regulator loop gain referred to the output approaches the ideal LQG regulator loop gain. This, in turn, requires that the LQG controller [5], given by

$$\mathbf{C}(s\mathbf{I}-\mathbf{A})^{-1}\mathbf{B}\mathbf{K}_c(s\mathbf{I}-(\mathbf{A}-\mathbf{L}\mathbf{C}-\mathbf{B}\mathbf{K}_c))^{-1}\mathbf{L} \Rightarrow \mathbf{C}(s\mathbf{I}-\mathbf{A})^{-1}\mathbf{L} \tag{6}$$

approaches the ideal LQG controller so as to recover all the robustness properties of the LQR controller [6]. When loop transfer recovery is achieved strictly, the poles of the closed loop tend to the zeros of the open-loop system, and this is not quite desirable as the zeros may lie in the right half of the complex plane as in nonminimum phase systems.

Clearly, the entire design depends critically on the availability of the noise covariance data. When such data are not available, one could adopt an LQR design method that enables the designer to achieve regulation performance with no constraints on the control effort. This is usually done by choosing the controller performance matrix $\mathbf{R}$, to be nonsingular and given by $\mathbf{R} = \varepsilon\mathbf{I}$ with $\varepsilon \to 0$ and choosing a diagonal $\mathbf{Q}$ so as to limit the maximum achievable values of state response magnitudes. In practice ε cannot be set to zero but is chosen to be small enough. Thus the closed-loop poles do not tend to the open-loop zeros but to a Butterworth [7] pattern, but only at the design point. We refer to a control law synthesized with these weightings as an unbounded or cheap control feedback law. On the other hand, to achieve regulation with minimum control effort, the controller performance matrix $\mathbf{R}$ must be nonsingular and given by $\mathbf{R} = \mathbf{I}$ while choosing a diagonal $\mathbf{Q} = \varepsilon\mathbf{Q}'$ with $\varepsilon \to 0$ so as to limit the *relative* maximum achievable values of state response magnitudes only. We refer to a control law synthesized with these weightings as a control weighted feedback law. A closed-loop system with such a control law is characterized by a symmetric root locus. The two extreme cases mentioned above very much characterize the limits of performance that can expected from various control law designs.

IV. Examples: Closed-Loop Stability Characteristics

One of the primary features we wish to demonstrate is that benefits of a continuous "smartly" excited flap are not entirely due to the distribution of the elastic stiffness. Rather they are substantially due to the absence of the aerodynamic singularity in the vicinity of the hinged flap's leading edge. Several examples and a number of parameter sets associated with each were considered. We now present an archetypal example of a 2 degrees of freedom fluttering airfoil to illustrate the features of both the open- and closed-loop characteristics. The first example considered is this traditional rigid airfoil with a trailing edge flap. In the first case considered the center of gravity was assumed to be aft of the elastic axis. In this case the airfoil exhibited flutter at a nondimensional airspeed of $\bar{U} = 45$ ($\bar{U}$ being the freestream velocity in semichords per second). Although the flutter could be alleviated by feedback control, it was first decided to attach a "tab" on a relatively stiff (but not rigid) mounting to illustrate the effects of flexibility distribution. Such a configuration does not really affect the singularity in the vicinity of the flap's leading edge. It is interesting to observe that the addition of the tab does not really influence flutter speed. This clearly illustrates that the flexibility by itself does not have a significant effect even when the system parameters are properly tuned. In the next example considered the airfoil was fitted with a continuous flexible trailing edge flap with flap width equal to 25% of the airfoil chord. The parameters of the airfoil were chosen to be the same as in the previous case while the flap was modeled as a cantilevered beam. This airfoil also exhibited flutter as in the case of the rigid airfoil but at a slightly higher airspeed of $\bar{U} = 75$. Interestingly, the simple addition of a stiffly mounted flexible flap provided adequate passive stabilization to raise the flutter speed to the higher value.

The flutter at the higher speed could be eliminated one of two ways: either by increasing the plunging natural frequency corresponding to the wing first bending natural frequency or by introducing feedback. In the latter case for the same design requirement which was to design the closed-loop control at $\bar{U} = 90$, and the closed-loop system with the control weighted feedback law showed no instability up to an airspeed of $\bar{U} = 200$ while there was a divergence at $\bar{U} = 100$ with the cheap control feedback law. In this case, although the open-loop system did not show any divergence, the closed-loop system revealed the divergence instability first. Although this was not exactly a case of control spillover, it illustrates the fact that there is no reason to assume that the closed-loop instabilities will be similar to the open-loop case. Thus in this case, representing the more robust of the control laws in that the robustness

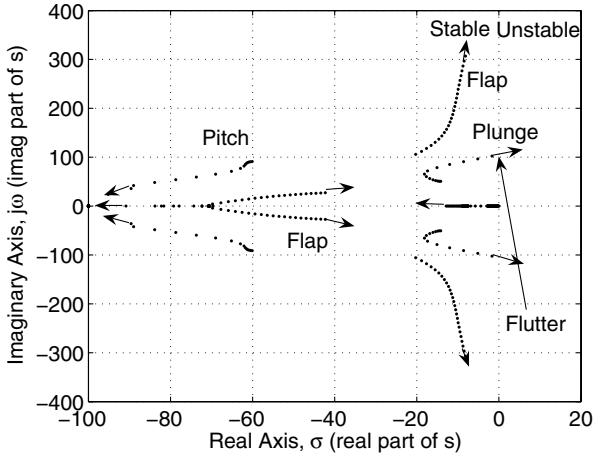

Fig. 1 The closed-loop root locus for the case of the open-loop fluttering airfoil with control weighted feedback, indicating closed-loop flutter at an airspeed of $\bar{U} = 200$.

properties of the LQR loop are largely recovered [5], the percentage increase in the first unstable flight speed is lower and yet significant.

Figure 1 illustrates the closed-loop root locus with respect to the parameter $\bar{U}$ (the arrows indicate the directions of the increasing airspeed parameter) including the control weight feedback law, and Fig. 2 shows the corresponding closed-loop root locus with the cheap control feedback law providing the control input. In Fig. 1, the plunge mode tends to instability with increasing speed, at an airspeed of $\bar{U} = 200$ while the torsion or pitching mode tends to be increasingly stable. The lag states remain on the real axis.

Based on the magnitudes of the gains associated with the states in the control law, the principal feedbacks quite closely corresponded to the dominant states in the flutter mode. The principal feedback control mode was the flap's first assumed polynomial mode. However, the second control mode played a significant yet secondary role with the cheap control feedback law. It may be recalled that it is indeed this control law that provides a more robust solution as it is in this case that the LQG regulator loop gain referred to the output approaches the ideal LQG regulator loop gain, so as to recover all the robustness properties of an LQR controller [5]. On this basis it can be concluded that the availability of multiple control modes provides for a robust closed-loop design.

Figure 3 illustrates a typical variation of the principal feedback gain associated with the nondimensional plunge displacement and the resulting percentage increase in the flutter speed from a typical baseline value. The gains are reasonable in magnitude indicating that the implementation of the control system is a feasible proposition. The actual value of the gain selected would depend on the control power available. The next significant feedback was the plunge rate

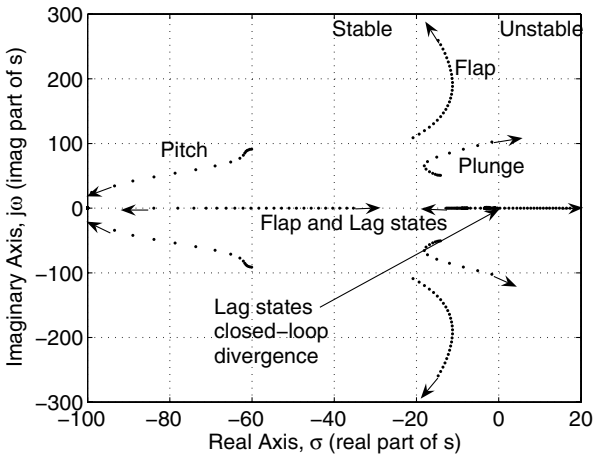

Fig. 2 The closed-loop root locus with the cheap control feedback law, indicating closed-loop divergence at $\bar{U} = 100$.

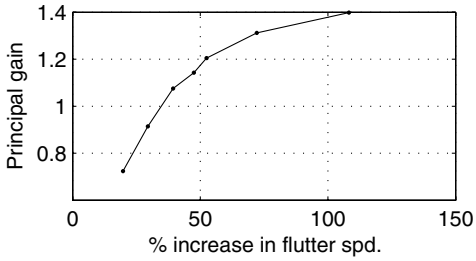

Fig. 3 Typical variation of the principal feedback gain associated with the nondimensional plunge displacement with the percentage increase in the flutter speed.

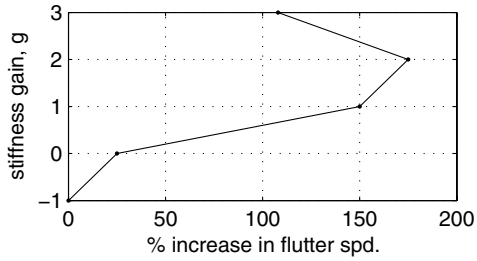

Fig. 4 Typical variation of the logarithmic stiffness gain, g, $K = 2g$ associated with the plunge degree of freedom with the percentage increase in the flutter speed.

and the associated feedback gain varied from about 0.4 to 0.8 of the primary gain. Figure 3 also illustrates another important feature of active flutter control that as the gain is increased, it approaches a critical steady limit, and the corresponding increase in the flutter speed is limitless, thus indicating that the phenomenon of flutter is completely alleviated. By contrast we may examine a passive method of flutter suppression by monotonically increasing the stiffness in the nondimensional plunge mode that is by far the parameter to which the open-loop flutter speed is most sensitive. The result is illustrated in Fig. 4. The figure illustrates the limited value of passive tuning in increasing the flutter speed beyond a certain limit. Similar results were obtained with other relevant parameters and groups of parameters. Thus the benefits of active control over passive parameter tuning are patently obvious when one compares Figs. 3 and 4.

From all the examples considered it was apparent that the provision for the smartly excited, continuous flap provides for greater controllability due to the availability of multiple flap modes although each individual flap mode was by itself not as effective as the articulated flap, partly due to the absence of the logarithmic singularity at the flap's leading edge. So it was clear that to fully realize the benefits of the continuous flap it must be employed as a multimode or multi-input controller. From a practical point of view one must necessarily be able to control flutter just by feeding back the measured states. Such an output feedback controller with an observer based compensator could be quite easily synthesized particularly from the cheap control feedback law.

VII. Conclusions

By far the most significant advantage of employing a smart flap to suppress flutter was the availability of multiple control modes for introducing the feedback. The various examples and the associated studies not only pointed to the fact that closed-loop designs involving a flexible flap were certainly more robust, but also that flutter can be more easily eliminated than by a rigid flap. The results obtained here not only vindicate the earlier results obtained by Nissim [2] employing a flap–tab combination but also indicate that the stabilization of a fluttering airfoil with a flexible flap is more easily achievable than by a rigid flap. Although in many cases it was found that active flutter suppression was possible in principle with a single control mode, the magnitudes of the feedbacks revealed that the

availability of a multitude of control modes made the design of a practical system much more feasible. Although the study was restricted to two, three, and four control modes, the first flap mode was found to be the most significant control mode in all cases. The principal feedbacks are almost always the primary states contributing to the flutter mode with the other states playing a secondary role.

References

[1] Theodorsen, T., and Garrick, I. E., "Non-Stationary Flow About a Wing-Aileron-Tab Combination Including Aerodynamic Balance," NACA TR 736, 1942.

[2] Nissim, E., "Active Flutter Suppression Using Trailing-Edge and Tab Control Surfaces," *AIAA Journal*, Vol. 14, No. 6, June 1976, pp. 757–762.

[3] Ashley, H., and Landahl, M. T., "Unsteady Flow," *Aerodynamics of Wings and Bodies*, Addison–Wesley, Reading, MA, 1965, Chap. 10; also available as a Dover paperback from Dover Publications, Inc., New York.

[4] Jones, R. T., "Operational Treatment of the Non-Uniform Lift Theory to Airplane Dynamics," NACA TN 667, March 1938, pp. 347–350.

[5] Burl, J. B., "Linear Quadratic Gaussian Control," *Linear Optimal Control: H_2 and H_8 Methods*, Addison Wesley Longman, Reading, MA, 1999, Chap. 8.

[6] Lewis, F. L., and Syrmos, V. L., "Robustness and Multivariable Frequency-Domain Techniques," *Optimal Control*, 2nd ed., Wiley, New York, 1995, Chap. 9.

[7] Bryson, A. E., Jr., "Some Connections Between Modern and Classical Control Concepts," *Journal of Dynamical Systems, Measurement, and Control*, Vol. 101, June 1979, pp. 91–98.